

# DLTS characterization of defects in GaN induced by electron beam exposure

P.N.M. Ngoepe,<sup>a)</sup> W.E. Meyer, F.D. Auret, E. Omotoso, and M. Diale

*Department of Physics, University of Pretoria, Private bag X20, Hatfield, 0028, South Africa*

## Abstract

The deep level transient spectroscopy (DLTS) technique was used to investigate the effects of electron beam exposure (EBE) on *n*-GaN. A defect with activation energy of 0.12 eV and capture cross section of  $8.0 \times 10^{-16} \text{ cm}^2$  was induced by the exposure. The defect was similar to defects induced by other irradiation techniques such as proton, electron, and gamma irradiation. In comparison to GaN, the EBE induced defects in other materials such as Si and SiC are similar to those induced by other irradiation methods.

*Keywords:* GaN, DLTS, electron beam exposure, defect

<sup>a)</sup>Corresponding author e-mail address: phuti.ngoepe@up.ac.za

## 1. Introduction

GaN is a wide bandgap ( $\approx 3.4$  eV) binary semiconductor which has been used in various applications because of its optical and electrical properties. These applications include detecting and emitting devices. The resistance to radiation damage has been one of the key factors in making it a suitable candidate for amongst other applications space applications. High energetic particles are known to induce electrically active defects in semiconductors. In particular, different processes, which are known to induce defects, have been investigated in a controlled environment. Doping is a process by which Cho *et al.* investigated the behavior of defects in intentionally and unintentionally doped *n*-GaN [1]. Various growth methods have been used to investigate deep levels in GaN. These include reactive molecular beam epitaxy (RMBE) [2], metal-organic vapour phase epitaxy (MOVPE) [3], hydride vapour phase epitaxy (HVPE) [4], and epitaxial lateral overgrowth (ELOG) [5]. A study of defects induced by etching using inductively coupled plasma (ICP) was performed by Nakamura *et al.* [6]. Auret *et al.* [7] investigated the introduction of defects by different metal deposition techniques. These included electro-deposition, sputter deposition, and electron beam deposition. It was reported by these authors that the deposition of metals using the electron beam deposition system induces defects in GaN. During metal deposition, the semiconductor is usually shielded until the metal is evaporated. In industrial applications, however, it may be difficult to shield the samples until just before evaporation. A novel method, termed electron beam exposure (EBE), has been explored by Coelho *et al.* [8] whereby Ge was exposed to electron beam deposition conditions without depositing the metals. This was with the view of investigating the effect that prolonged exposure of the samples to deposition conditions would have on the defect properties of the sample. In this study, we investigate the effect of electron beam exposure on GaN using DLTS.

## 2. Experimental

The study was performed on a Si doped *n*-type GaN wafer which was grown by HVPE. This wafer had a carrier concentration of  $1 \times 10^{17} \text{ cm}^{-3}$ . The GaN wafer was degreased by boiling in trichloroethylene and isopropanol for 3 min. each. Boiling aqua regia was used to etch the sample for 10 min. After each cleaning step, the sample was rinsed 3 times in de-ionised water. An HCl:H<sub>2</sub>O solution was then used as the last etching step. Thereafter the sample was blown dry with N<sub>2</sub>. Ohmic contacts consisting of Ti (150 Å)/Al (2200 Å)/Ni (400 Å)/Au (500 Å) were deposited using the electron beam evaporation system. The ohmic contacts were annealed for 5 min. in flowing Ar. Prior to loading the sample in the electron beam system, the sample was dipped in an HCl:H<sub>2</sub>O solution to remove contaminants that might have formed on the surface. The sample was then placed in the electron beam chamber. There are two main sources of particles in an electron beam system. These included particles that are released from the filament from which the electrons are accelerated onto the target metal and also particles which are evaporated from the metals being deposited. The electron gun was shielded from the target sample. This was done to reduce stray particles from the electron gun that might impinge on the sample. Whilst in the electron beam system chamber, the sample was exposed to electron beam conditions without evaporating any metals. A crucible containing tungsten was heated at a current of 100 mA for exposure times of 50 and 80 min. Tungsten was used as a target metal due to its high melting point (3422 °C). It can simulate electron beam deposition conditions of metals with lower melting points without evaporation. Ni (250 Å)/ Au (650 Å) Schottky contact was deposited using a resistive evaporation system, a process that is known not to introduce electrically active defects in measurable quantities. One sample was subjected to EBE while another sample was used as a reference. Current-voltage characteristics were performed in order to verify the suitability of the Schottky contact for deep level transient spectroscopy (DLTS) measurements. Conventional DLTS

was then employed to measure the defects before and after exposure. The DLTS measurements were performed by a computer controlled system with a closed cycle helium cryostat and a 1 MHz Boonton 7200 capacitance meter.

### **3. Results and discussion**

The DLTS spectra of the control and EBE samples are compared in Fig. 1. The DLTS spectra were measured using a reverse bias voltage of -1 V, a filing pulse height of 0.2 V and a filing pulse width of 2 ms. The reverse bias voltage was relatively small in order to probe the space charge region close to the surface of the metal-semiconductor contact. The rate window of the measured spectra was  $80 \text{ s}^{-1}$ . A comparison is made for a temperature range of 70 and 200 K as the spectra beyond these temperatures are the same. The DLTS spectrum shows that a defect is induced at a peak temperature of 100 K after EBE. The Arrhenius plot of the defects before and after exposure is shown in Fig. 2. Table 1 compares the EBE induced defect to other irradiation induced defects. The activation energy of the EBE induced defect and the apparent capture cross section are 0.12 eV and  $8.0 \times 10^{-16} \text{ cm}^2$  respectively. These parameters were extracted from a multirate window scan of the DLTS spectra.

The EBE induced defect is a bulk defect in the semiconductor near the surface of the metal-semiconductor interface. The distinction between bulk traps and interface states is that the peak maximum of the DLTS signal of bulk traps does not move or moves towards lower temperatures whereas the peak maximum of interface states moves towards higher temperatures with increasing pulse height. In our study we observed that the peak maximum of the DLTS signal does not move with respect to the temperature when we increase the pulse height by changing the reverse bias voltage.

**Fig. 1.** DLTS spectra comparing the control sample spectrum to the EBE spectrum.

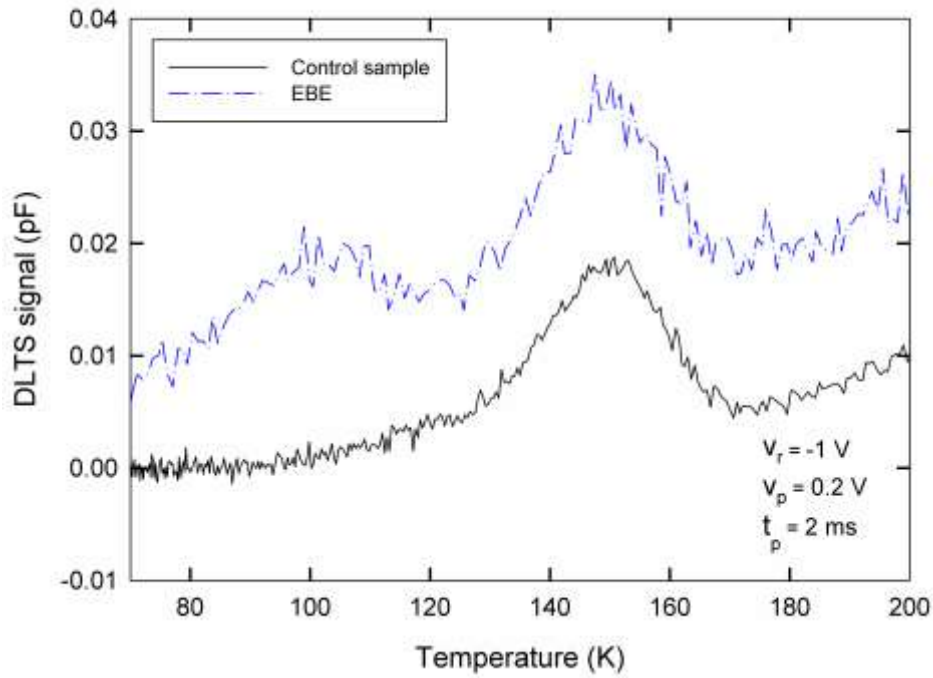


**Fig. 2.** Arrhenius plots of Ni/Au diodes which were resistively evaporated on GaN. One sample was subjected to EBE while the other was used as a control sample.

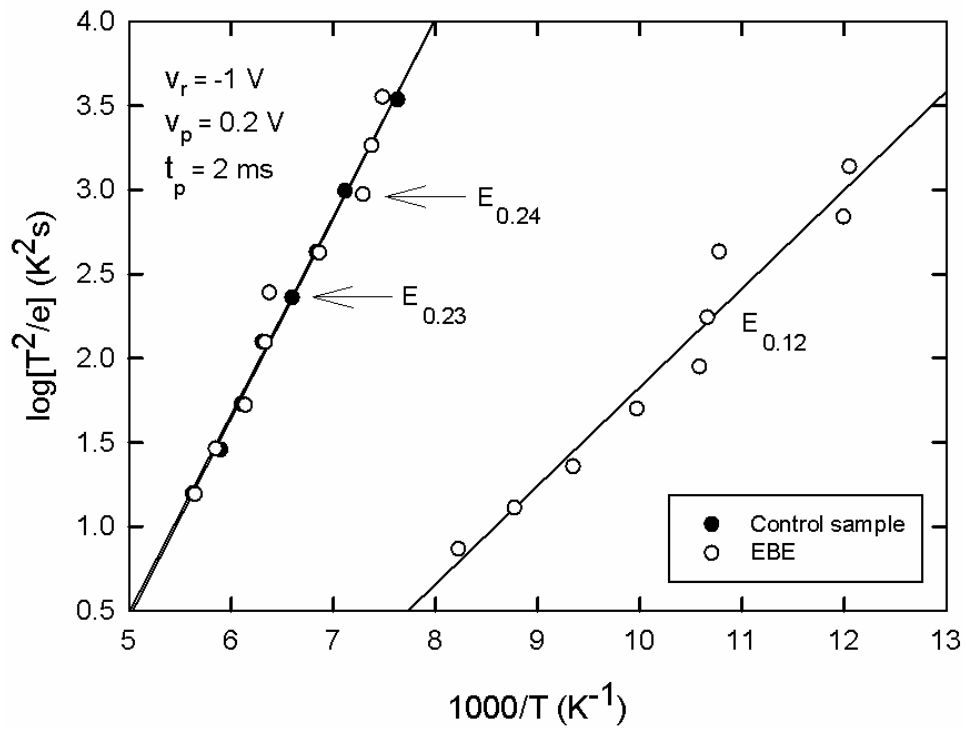


**Table 1.** Comparison of defects induced by the EBE technique and different irradiation methods.

Process	Defect label	Defect level (eV)	Apparent capture cross section (cm <sup>2</sup> )	Peak Temperature (K)	Similar defects/ Ref.
Electron beam exposure	E <sub>0.12</sub>	0.12	$8.0 \times 10^{-16}$	100	
0.2 - 2.4 MeV electron irradiation	ER1	0.13	-	98	[9]
2.0 MeV proton irradiation	ER1	0.13	-	98	[9]
1.8 MeV proton irradiation	-	0.13	$1 \times 10^{-17}$	100	[10]
24 GeV proton irradiation	T1	0.12	$1.3 \times 10^{-17}$		[11]
<sup>60</sup> Co gamma irradiation	G <sub>A</sub>	0.13	$4.9 \times 10^{-18}$		[12]

The activation energy of the EBE defect is similar to the activation energy of the ER1 defect reported by Goodman *et al.* [9]. In their study they irradiated GaN with electrons and protons. Zhang *et al.* and Castaldini *et al.* also irradiated GaN with protons [10,11]. The activation energies of the induced defects in their studies were 0.13 and 0.12 eV respectively. The proton irradiation was done with different irradiation energies namely 1.8 MeV and 24 GeV. Umana-Membreno *et al.* subjected undoped *n*-type GaN to <sup>60</sup>Co gamma irradiation and also found a defect similar to the EBE induced defect [12]. The gamma irradiation induced defect had activation energy of 0.13 eV. In their study, Umana-Membreno *et al.* also observed that the defect is significantly insensitive to fluence rate. This observation was comparable to gamma particle radiation investigated by Schmidt *et al.* [13]. The concentration of the defect induced by EBE was not affected by exposure time beyond 50 min. The sample was first exposed to electron beam conditions for 50 min. After exposure for an additional 30 min., the

concentration of the defect remained relatively unchanged. It seems that saturation is reached after 50 min. exposure. We speculate that the defect might be a complex between a mobile irradiation induced defect and an immobile as-grown defect, that might not be electrically active. One would therefore expect the concentration of the complex to increase until all as-grown defects have reacted, after which the concentration will level off. The concentration of the EBE induced defect was  $2.6 \times 10^{13} \text{ cm}^{-3}$ .

A comparison of different metallisation techniques is tabulated in Table 2. The activation energy of the EBE induced defect is smaller than the activation energies of the defects induced by electron beam and sputter deposition. These two deposition techniques induced defects with activation energies of 0.19 eV [14] and 0.22 eV [15] respectively. Other defects induced by these two methods had higher activation energies.

**Table 2.** Comparison between the defect induced by the EBE and different metallisation techniques.

Process	Defect label	Defect level (eV)	Apparent capture cross section ( $\text{cm}^2$ )	Peak Temperature (K)	Similar defects/ Ref.
Electron beam exposure	$E_{0.12}$	0.12	$8.0 \times 10^{-16}$	100	
Electron beam deposition	Ee1	0.19	$1.2 \times 10^{-15}$	120	[14]
Sputter deposition	ES1	0.22	$6.5 \times 10^{-16}$	120	[15]

In the electron beam deposition (EBD) study, Auret *et al.* speculated that some ionised atoms, possibly from the evaporated metal and residual gasses in the vacuum chamber, reached the surface of the semiconductor with sufficient energy to damage the sample [14]. During the EBE method, W was heated but not deposited onto the semiconductor. This produced the conditions under which the radiation induced damage occurred for long enough to ensure that

a measureable concentration of defects was formed before a metal layer was deposited (effectively screening the semiconductor from further damage). Since metals were evaporated during EBD, the ionised atoms from these metals and other atoms with which subsequent collisions occurred, could gain sufficient energy to cause more damage on the EBD samples than the EBE samples.

The as grown defect increased in concentration by approximately a factor of 2 from  $2.4 \times 10^{13} \text{ cm}^{-3}$  to  $4.5 \times 10^{13} \text{ cm}^{-3}$ . The activation energies of the control and EBE sample of this defect are 0.23 and 0.24 eV respectively. This defect has been reported by various authors. It has been observed in GaN grown with different methods such as HVPE, MOVPE, ELOG, and RMBE [16].

Other DLTS studies have been performed on different semiconductor materials using the EBE method. Danga *et al.* reported that in Si, the defect induced was similar to defects induced by proton and alpha particle irradiation [17]. In 4H-SiC, Omotoso *et al.* observed that the defects induced by EBE are similar to those induced by alpha particle and high-energy electron irradiation [18]. Coelho *et al.* reported that to the best of their knowledge, none of the EBE induced defects in Ge had been reported before [8]. It is interesting to note that apart from Ge, the defects induced by EBE in other semiconductor materials are similar to defects induced by different irradiation methods. This is also consistent with the findings performed on GaN in this study.

#### **4. Conclusion**

Electron beam exposure induced a defect with activation energy of 0.12 eV in GaN. This defect is similar to other defects induced by different irradiation methods including electron, proton and gamma particle irradiation. The activation energy of the EBE induced defect was much lower than other defects induced by different metal deposition techniques. EBE can

thus be another method of introducing the 0.12 eV defect. The as grown defects in the sample were not significantly affected by EBE. A comparison of different semiconductors subjected to EBE indicates that, except for Ge, the EBE induced defects are similar to other irradiation induced defects.

### **Acknowledgements**

The authors would like to acknowledge the South African National Research Foundation (NRF) (Grant No. 99861) for the financial support during this study.

## References

- [1] H.K. Cho, C.S. Kim, and C.-H. Hong, *J. Appl. Phys.* **94**, 1486 (2003).
- [2] Z-Q. Fang, D. C. Look, W. Kim, Z. Fan, A. Botchkarev and H. Morkoc, *Appl. Phys. Lett.* **72**, 2277 (1998).
- [3] P. Hacke, A. Maekawa, N. Koide, K. Hiramatsu, and N. Sawaki, *Jpn. J. Appl. Phys.* **33**, 6443 (1994).
- [4] D.C. Look, Z.-Q. Fang, and B. Claflin, *J. Crystal Growth* **281**, 143 (2005).
- [5] In-Hwan Lee, A.Y. Polyakov, N.B. Smirnov, A.V. Govorkov, A.V. Markov, and S.J. Pearton, *Thin Solid Films* **516**, 2035 (2008).
- [6] W. Nakamura, Y. Tokuda, H. Ueda, and T. Kachi, *Physica B* **376–377**, 516 (2006).
- [7] F.D. Auret, S.A. Goodman, G. Myburg, S.E. Mohnney, and J.M. de Lucca, *Mater. Sci. Eng.* **B82**, 102 (2001).
- [8] S.M.M. Coelho, F.D. Auret, P.J. Janse van Rensburg, and J.M. Nel, *J. Appl. Phys.* **114**, 173708 (2013).
- [9] S.A. Goodman, F.D. Auret, F.K. Koschnick, J.M. Spaeth, B. Beaumont, and P. Gibart, *Mater. Sci. Eng.* **B71**, 100 (2000).
- [10] Z. Zhang, E. Farzana, W.Y. Sun, J. Chen, E.X. Zhang, D.M. Fleetwood, R.D. Schrimpf, B. McSkimming, E.C.H. Kyle, J.S. Speck, A.R. Arehart and S.A. Ringel, *J. Appl. Phys.* **118**, 155701 (2015).
- [11] A. Castaldini, A. Cavallini, and L. Polenta, *J. Phys.: Condens. Matter.* **12**, 10161 (2000).
- [12] G.A. Umana-Membreno, J.M. Dell, T.P. Hessler, B.D. Nener, G. Parish, L. Faraone, and U.K. Mishra, *Appl. Phys. Lett.* **80**, 4354 (2002).
- [13] N.M. Shmidt, D.V. Davydov, V.V. Emtsev, I.L. Krestnikov, A.A. Lebedev, W.V. Lundin, D. S. Poloskin, A. V. Sakharov, A. S. Usikov, and A. V. Osinsky, *Phys. Stat. Sol. (b)* **216**, 533 (1999).
- [14] F.D. Auret, S.A. Goodman, G. Myburg, F.K. Koschnick, J.M. Spaeth, B. Beaumont, and P. Gibart, *Physica B* **273-274**, 84 (1999).
- [15] F.D. Auret, W.E. Meyer, S.A. Goodman, F.K. Koschnick, J.M. Spaeth, B. Beaumont, and P. Gibart, *Physica B* **273-274**, 92 (1999).
- [16] F.D. Auret, S.A. Goodman, G. Myburg, W.E. Meyer, J.M. Spaeth, P. Gibart and B. Beaumont, *Radiation Effects & Defects in Solids* **156**, 255 (2001).
- [17] H.T. Danga, F.D. Auret, S.M.M. Coelho, and M. Diale, *Physica B* **480**, 206 (2016).
- [18] E. Omotoso, W.E. Meyer, F.D. Auret, S.M.M. Coelho, and P.N.M. Ngoepe, *Solid State Phenomena* **242**, 427 (2016).